

# Viscoelastic contact mechanics between randomly rough surfaces

M. Scaraggi<sup>1,2</sup> and B.N.J. Persson<sup>2</sup>

<sup>1</sup>*DII, Università del Salento, 73100 Monteroni-Lecce, Italy, EU and*

<sup>2</sup>*PGI, FZ-Jülich, 52425 Jülich, Germany, EU*

We present exact numerical results for the friction force and the contact area for a viscoelastic solid (rubber) in sliding contact with hard, randomly rough substrates. The rough surfaces are self-affine fractal with roughness over several decades in length scales. We calculate the contribution to the friction from the pulsating deformations induced by the substrate asperities. We also calculate how the area of real contact,  $A(v, p)$ , depends on the sliding speed  $v$  and on the nominal contact pressure  $p$ , and we show how the contact area for any sliding speed can be obtained from a universal master curve  $A(p)$ . The numerical results are found to be in good agreement with the predictions of an analytical contact mechanics theory.

Viscoelastic solids, such as rubber or gel, have many important applications in science and technology. Rubber friction, for example, is a topic of great practical importance e.g., for tires, syringes, wiper blades or rubber seals, and it results from dissipative processes involving multiple (coupled) nano- to micro- (or more) length scales, which are related to the relaxation and diffusion dynamics of the confined polymers[1–4] as well as to the random interaction process[5] occurring in real interfaces. Due to the (numerical) complexity of the under-

theory with experimental results is an important benchmark for any theory validation process, but the superposition of coupled dissipation mechanisms encountered in rubber friction make it very hard to test separately the different contributions to the rubber friction. Hence, in this context any exact numerical calculations under well defined contact characteristics, even if only possible for relatively-small systems under idealized conditions, can furnish very useful insights into the processes occurring in rubber sliding contacts, and test analytical theories.

In this work we make an attempt to shed light on the mechanisms of micro-rolling friction and contact area formation in the interaction between randomly rough surfaces of viscoelastic solids. In particular, we will compare the exact numerical results with the predictions of the (more general) Persson's contact mechanics theory. We use a recently developed residuals molecular dynamics (RMD[9]) scheme, adapted to the rubber viscoelastic rheology. The RMD method has so far has been successfully applied to the investigation of adhesive contacts between elastic solids with random roughness[10], and here we extend the study to the case of sliding contact between linear viscoelastic solids with random surface roughness. The RMD numerical model is based on a (finite element) formulation in wavevector space, together with a molecular dynamics modelling of the interfacial separation in real space, the latter driven by the residuals of the discretized contact mechanics equations. This (general-purpose) approach allows for an equally efficient computation of the contact dynamics from very small values of contact areas up to full contact interactions.

One of us[5] has derived a set of equations describing the friction force acting on a rubber block sliding at the velocity  $v(t)$  in contact with a hard substrate with randomly rough surface [5]. For a rubber in dry contact with a hard solid with a rough surface there are two main contributions to rubber friction, namely (i) a contribution derived from the energy dissipation inside the rubber due to the pulsating deformations it is exposed to during sliding (it could be named micro-rolling friction, as it shares the dissipation mechanism with the classical rolling friction), and (ii) a contribution from the shear-

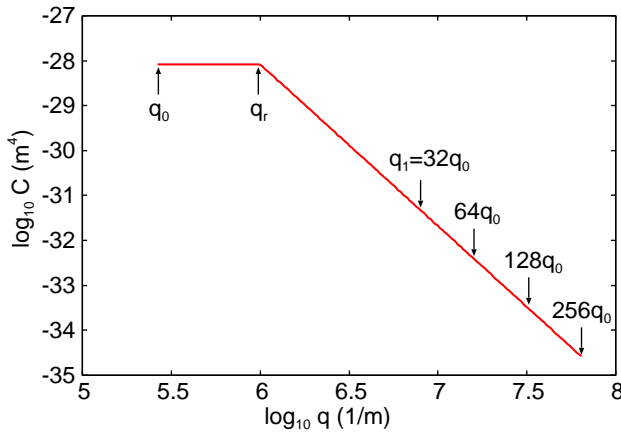


Figure 1: Surface roughness power spectra used in the present study. The power spectra have a low wavevector cut-off for  $q_0 = 0.25 \times 10^6 \text{ m}^{-1}$ , and a roll-off for  $q_r = 4q_0$ . For  $q > q_r$  the power spectra correspond to a self-affine fractal surface with the Hurst exponent  $H = 0.8$ . We consider 4 cases where the large wavevector cut-off is  $q_1 = 32q_0$ ,  $64q_0$ ,  $128q_0$  and  $256q_0$ ; we refer to  $q_1 = 32q_0$  and  $256q_0$  as the small and large system, respectively. In the numerical calculations, a null power spectrum region is added between  $q_1$  and  $\bar{q}_1 = 8q_1$  to improve convergence.

lying contact mechanics problem[6, 7], involving multiple length and time scales, the friction force as well as the real contact area between viscoelastic solids under real contact conditions has so far only been predicted using mean field formulations of the contact mechanics, such as the one by Persson[5] or Klüppel and Heinrich[8]. Comparing

ing processes occurring in the area of real contact. For sliding at a constant velocity  $v$ , and neglecting frictional heating, the friction coefficient due to process (i) is:

$$\mu \approx \frac{1}{2} \int_{q_0}^{q_1} dq q^3 C(q) S(q) P(q) \times \int_0^{2\pi} d\phi \cos \phi \operatorname{Im} \frac{E(qv \cos \phi)}{(1 - \nu^2) \sigma_0}, \quad (1)$$

where  $\sigma_0$  is the nominal contact stress,  $C(q)$  the surface roughness power spectrum and  $E(\omega)$  the rubber viscoelastic modulus. The function  $P(q) = A(\zeta)/A_0$  is the relative contact area when the interface is observed at the magnification  $\zeta = q/q_0$ , where  $q_0$  is the smallest (relevant) roughness wavevector. We have

$$P(q) = \frac{2}{\pi} \int_0^\infty dx \frac{\sin x}{x} \exp[-x^2 G(q)] = \operatorname{erf} \left( \frac{1}{2\sqrt{G}} \right) \quad (2)$$

where

$$G(q) = \frac{1}{8} \int_{q_0}^q dq q^3 C(q) \int_0^{2\pi} d\phi \left| \frac{E(qv \cos \phi)}{(1 - \nu^2) \sigma_0} \right|^2 \quad (3)$$

The factor  $S(q)$  in (1) is a correction factor which takes into account that the asperity-induced deformations of the rubber is smaller than would be in the case if complete contact would occur in the (apparent) contact areas observed at the magnification  $\zeta = q/q_0$ . For contact between elastic solids this factor reduces the elastic asperity-induced deformation energy, and including this factor gives a distribution of interfacial separation in good agreement with experiment and exact numerical studies[11]. The interfacial separation describes how an elastic (or viscoelastic) solid deforms and penetrates into the roughness valleys, and it is stressed here that these (time-dependent) deformations cause the viscoelastic contribution to rubber friction. We assume that the same  $S(q)$  reduction factor as found for elastic contact is valid also for sliding contact involving viscoelastic solids. For elastic solids it has been found that  $S(q)$  is well approximated by

$$S(q) = \gamma + (1 - \gamma) P^2(q),$$

where  $\gamma \approx 1/2$ , and here we use the same expression for viscoelastic solids, being in nature a geometrical parameter. Note that  $S \rightarrow 1$  as  $P \rightarrow 1$  which is an exact result for complete contact. In fact, for complete contact the expression (1) is exact (see below). Note finally that in the original rubber friction theory[5] the correction factor  $S(q)$  was not included.

The second contribution (ii) to the rubber friction force, associated with the area of (apparent) contact observed at the magnification  $\zeta_1 = q_1/q_0$ , is given by  $\tau_f A_1$ . Here,  $\tau_f(v)$  is the (weakly) velocity-dependent effective frictional shear stress acting in the contact area

$A_1 = A(\zeta_1) = P(q_1) A_0$ . In this study we only consider the viscoelastic contribution to the rubber friction, but we also study the area of real contact which is needed when calculating the second contribution to the rubber friction.

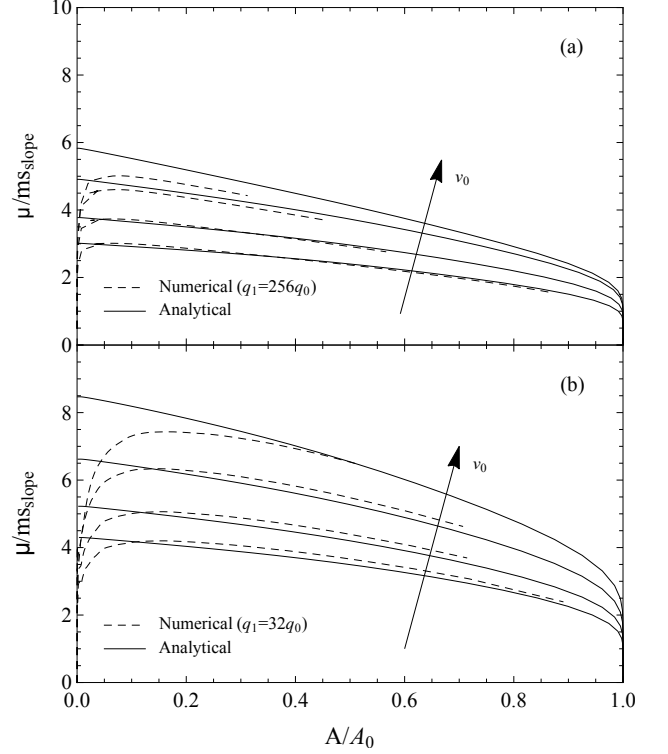


Figure 2: The friction coefficient, divided by the ms slope, as a function of the (normalized) area of contact  $A/A_0$ , for several sliding speeds:  $v = 0.01, 0.1, 1, 10$  m/s. The solid lines are the theory predictions, while the dotted lines are from the exact numerical study. for (a) large system, and (b) small system.

Note that the surface mean square slope is given by

$$\langle (\nabla h)^2 \rangle = 2\pi \int_{q_0}^{q_1} dq q^3 C(q)$$

so we can write

$$\frac{\mu}{\langle (\nabla h)^2 \rangle} \approx \frac{\int_{q_0}^{q_1} dq q^3 C(q) S(q) P(q) \int_0^{2\pi} d\phi \cos \phi \operatorname{Im} \frac{E(qv \cos \phi, T_0)}{(1 - \nu^2) \sigma_0}}{4\pi \int_{q_0}^{q_1} dq q^3 C(q)}. \quad (4)$$

For complete contact  $S(q) = P(q) = 1$  and if  $\operatorname{Im} E(\omega, T_0)$  would be weakly dependent on  $\omega$ , the integral over  $\phi$  in (4) would be weakly dependent on  $q$ , and in this limiting case the viscoelastic friction coefficient would be nearly proportional to the mean square slope. However, these assumptions never holds in practice and the friction

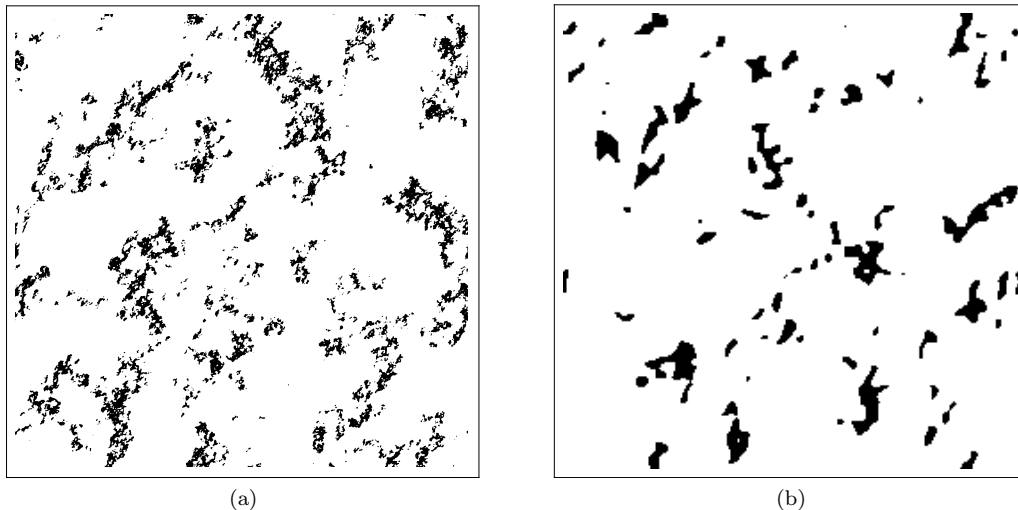


Figure 3: The contact morphology for the sliding speed  $v = 10$  m/s and for such a normal load that  $A/A_0 \approx 0.05$ . (a) large system, (b) small system. Black domains correspond to the true contact area.

coefficient cannot be simply related to the mean surface slope.

We now present exact numerical results for the viscoelastic contribution to the friction for a wide range of contact conditions, including nominal contact pressure, sliding velocity, and the large wavevector cut-off  $q_1$  (which determines the length scales over which the surface exhibit roughness). The RMD numerical results will be compared with the predictions of the rubber friction theory presented above.

In the calculations we use the viscoelastic modulus  $E(\omega)$  measured for a tread rubber compound[12], and the substrate is assumed rigid with a randomly rough isotropic surface. Fig. 1 shows the surface roughness power spectra used in the present study. The power spectra have a low wavevector cut-off for  $q_0 = 0.25 \times 10^6 \text{ m}^{-1}$ , and a roll-off for  $q_r = 4q_0$ . For  $q > q_r$  the power spectra correspond to a self-affine fractal surfaces with the Hurst exponent  $H = 0.8$ . We consider four cases where the large wavevector cut-off is  $q_1 = 32q_0$ ,  $64q_0$ ,  $128q_0$  and  $256q_0$ ; we refer to  $q_1 = 32q_0$  and  $256q_0$  as the small and large system, respectively. The root mean square roughness is determined mainly by the long-wavelength roughness and is therefore nearly the same for all the different cases, with  $h_{\text{rms}} \approx 27 \text{ nm}$ .

Figures 2a and 2b show the friction coefficients [divided by the mean square (ms) slope], as a function of the (normalized) area of contact  $A/A_0$ , for the large and small systems, respectively, and for several sliding speeds:  $v = 0.01, 0.1, 1, 10$  m/s. The solid lines are the predictions of the Persson's rubber friction theory, whereas the dotted lines are from the exact numerical study. Note that because of the Hertzian-like contact for small load, the numerical friction curves show a non-monotonic be-

haviour, where friction increases at small increasing values of contact areas. For high enough loads the friction coefficient decreases with increasing load (corresponding to increasing contact area) and the numerical results smoothly converge to the mean field predictions. Note that at  $A/A_0 \approx 0.05$ , the small system is still in the Hertzian friction regime[13], whereas the large system is experiencing the transition. Fig. 3(a) and 3(b) show the contact morphology for  $A/A_0 \approx 0.05$  for both the large and small systems, respectively, at sliding speed  $v_0 = 10$  m/s. For the large system the contact is split in a huge number of smaller patches (compared to the small system). When the surface exhibits roughness at shorter and shorter length scales (i.e. when the cut-off  $q_1$  increases) the Hertzian-like contact will prevail only at lower and lower nominal contact pressure, i.e. the finite size effect will be confined at smaller nominal contact areas and the system will move toward the thermodynamic limit, where a remarkably good agreement with the mean field theory exists.

Fig. 4 shows the (normalized) area of real contact as a function of the applied pressure  $p_N$  [divided by the root mean square (rms) slope], for several values of roughness cut-off wavevectors ( $q_1 = 32q_0$ ,  $64q_0$ ,  $128q_0$  and  $256q_0$ ) and sliding velocities ( $v = 1, 10$  m/s). In particular, the solid lines are the theory results and the dotted lines are from the numerical simulations. The agreement is very good. It is observed that when the sliding velocity increases, the asperity deformation frequencies increase and the rubber becomes elastically stiffer, resulting in the decrease of the contact area with increasing sliding speed. Moreover, this local stiffening depends on the perturbing frequencies which increases when more short-wavelength roughness is added to the surface profile, i.e., when  $q_1$

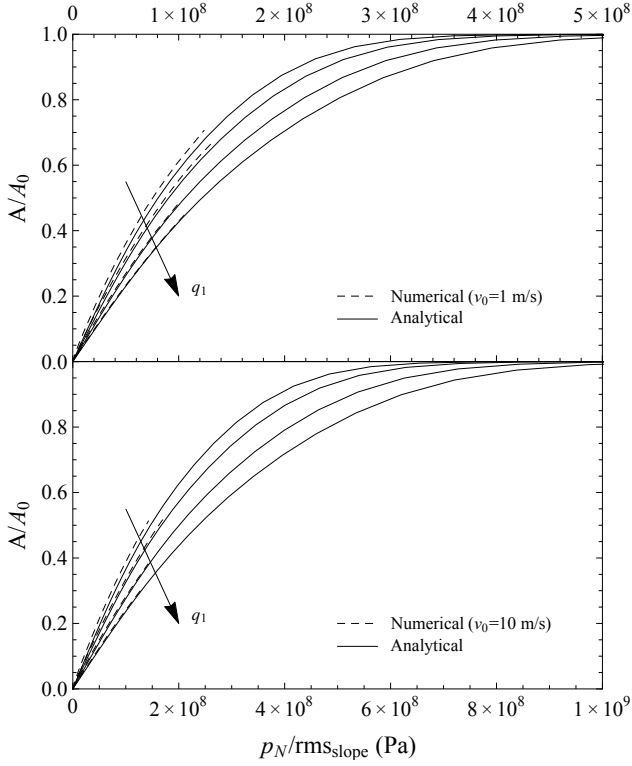


Figure 4: The normalized area of contact  $A/A_0$  as a function of the contact pressure  $p_N$  (divided by the rms slope), for several large cut-off frequencies  $q_1$ . The reported values correspond to sliding velocities occurring in the rubbery-to-glassy rubber transition regime.

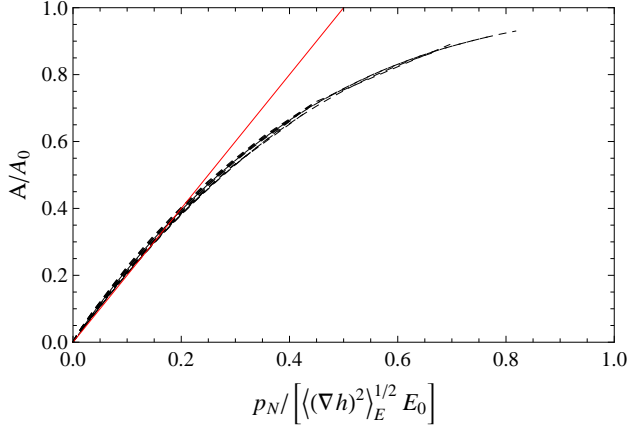


Figure 5: The numerically-calculated nominal contact area  $A/A_0$  as a function of the contact pressure  $p_N / [\langle (\nabla h)^2 \rangle_E^{1/2} E_0]$  [where  $\langle (\nabla h)^2 \rangle_E^{1/2}$  is an effective mean-square surface slope defined in (6)], for several values of roughness cut-off wavevectors ( $q_1 = 32q_0, 64q_0, 128q_0$  and  $256q_0$ ) and sliding velocities ( $v = 0.01, 0.1, 1, 10$  m/s). All the curves appear superposed to an unique mastercurve. The red line has a slope of 2.

increases. Therefore, for viscoelastic contacts one can-

not expect the area of real contact to be proportional to the inverse of the the root-mean-square roughness as observed for elastic contacts. This is confirmed by Fig. 4 which shows that for each velocity value, the numerically-predicted curves are not superposing, in agreement with the analytical results (2).

However, the analytical theory (2) and (3) suggests a possible mechanism to interpret the contact area results. As shown in Eq. (3), this local (scale dependent) rubber stiffening is equivalent to an apparent increase (with respect to the static contact) of the roughness power spectral content by a factor

$$s(q, v_0) = \frac{1}{2\pi} \int_0^{2\pi} d\phi \left| \frac{E(qv \cos\phi, T_0)}{E_0} \right|^2, \quad (5)$$

where  $E_0$  is the low frequency rubber elastic modulus [ $E_0 = E(\omega \rightarrow 0)$ ]. Hence, it is now easy to define a new (viscoelastic-dependent) effective mean square slope as

$$\langle (\nabla h)^2 \rangle_E = 2\pi \int_{q_0}^{q_1} dq q^3 C(q) s(q, v), \quad (6)$$

which is depending on the sliding velocity  $v$  via the dependency of  $E(\omega)$  on  $\omega = qv \cos\phi$ . In Fig. 5 we shown the normalized contact area as a function of the contact pressure scaled by the effective root mean square slope, for several values of roughness cut-off wavevectors ( $q_1 = 32q_0, 64q_0, 128q_0$  and  $256q_0$ ) and sliding velocities ( $v = 0.01, 0.1, 1, 10$  m/s). Remarkably, the theory-suggested scaling allows to obtain an unique contact mastercurve similar to the case of purely elastic interactions. Hence, it is recognizable that an universal scaling rules the asperity mediated multiscale interaction of randomly rough surfaces, which is insensitive to the particular rheological description of the bulk dynamics.

To summarize, we have performed exact numerical calculations for the viscoelastic contribution to rubber friction, and compared the results with the prediction of an analytical theory. Both the friction coefficient and the area of contact are rather well described by the theory, in particular for large contact pressure (in the limit of complete contact, the analytical theory is exact). Viscoelasticity will introduce some anisotropy in the contact morphology, but this effect seems to be rather unimportant for the variation of the rubber friction and contact area with sliding speed. In the numerical calculations we have neglected the effect of frictional heating and strain softening, which are likely to be important in most practical applications. These effects can be approximately included in the analytical theory, but including the same effects in the numerically exact treatment seems highly non-trivial.

**Acknowledgments** MS acknowledges FZJ for the support and the kind hospitality received during his visit to the PGI-1, where this work was initiated. MS also

acknowledges COST Action MP1303 for grant STSM-MP1303-090314-042252.

- 
- [1] K.A. Grosch, Proc. R. Soc. London, Ser. **A274**, 21 (1963)
  - [2] A. Schallamach, Wear **6**(5), 375-382 (1963)
  - [3] K.C. Ludema, D. Tabor, Wear **9**(5), 329-348 (1966)
  - [4] J.D. Ferry, *Viscoelastic properties of polymers*, 3rd edn. (Wiley, 1980)
  - [5] B.N.J. Persson, J. Chem. Phys. **115**, 3840 (2001)
  - [6] B.N.J. Persson, O. Albohr, U. Tartaglino, A.I. Volokitin, E. Tosatti, J. Phys.: Condens. Matter **17**(1), R1-R62 (2005)
  - [7] G. Carbone, C. Putignano, Phys. Rev. E **89**(3), 032408 (2014)
  - [8] M. Klüppel and G. Heinrich, Rubber Chem. Technol. **73**, 578 (2000)
  - [9] M. Scaraggi, *in preparation* (2014)
  - [10] B.N.J. Persson, M. Scaraggi, *submitted*, arXiv:1405.3123 [cond-mat.soft], (2014)
  - [11] A. Almqvist, C. Campana, N. Prodanov, B.N.J Persson, J. Mech. Phys. Solids **59**, 2355 (2011)
  - [12] B. Lorenz and B.N.J. Persson (unpublished)
  - [13] J. Greenwood, D. Tabor, J. Phys. Soc. **71**, 989 (1958)